Interception, throughfall, and snowpack dynamics in western juniper: Potential impacts of climate change and shifts in semi-arid vegetation

Ryan J. Niemeyer[1], Timothy E. Link[1,2], Mark S. Seyfried[3], and Gerald N. Flerchinger[3]

[1]Water Resources Program, University of Idaho, Moscow, ID 83843, USA

[2] Dept. of Forest, Rangeland, and Fire Sciences, University of Idaho, Moscow, ID 83843, USA

[3]USDA-Agricultural Research Service, Northwest Watershed Research Center, Boise, ID 83712, USA

Financial support was provided by the National Science Foundation's IGERT Program (Award 0903479) and by the National Science Foundation's CBET Program (Award 0854553).

Mention of a proprietary product does not constitute a guarantee or warranty of the product by USDA or the authors and does not imply its approval to the exclusion of the other products that also may be suitable.

ABSTRACT

Shifts in both climate and land cover can both potentially impact above ground hydrological processes. In the western U.S., both climatic shifts from snow to rain-dominated precipitation and land cover shifts of pinyon and juniper species in grass and shrub-dominated landscapes alter interception, throughfall and snowpack dynamics. To better understand how shifts in both vegetation cover and precipitation phase alter above-ground hydrological processes, we assessed differences in rain interception, and snow and rain throughfall in western juniper, how western juniper alters snowpack dynamics, and how these above-ground processes differ across western juniper, mountain big sagebrush, and low sagebrush plant communities. We collected continuous throughfall with four large lysimeters, continuous interspace and below-canopy snow depth data, and conducted periodic snow surveys for two consecutive water years (2013 and 2014). Throughfall, estimated with the lysimeter data, was greater for snow relative to rain events, averaging 74.9% and 54.8% respectively. We validated the Simultaneous Heat and Water (SHAW) model with eight years of continuous snow depth data, two years of interspace and canopy snow depth data, and interspace and canopy lysimeter data. We then simulated above-ground energy and water fluxes for an eight year period with more hydrometerological variability. We simulated surface water fluxes in western juniper, low sagebrush, and mountain big sagebrush cover under both the current and a mid-21st century ensemble projected climate. Comparison of the simulations revealed that changes in vegetation principally change the amount of hydrological fluxes such as surface water input, while the future (warmer) climate alters the timing of those fluxes.

Information from this study can help managers understand how both shifts in climate and semi-arid vegetation will alter fundamental hydrological processes.

INTRODUCTION

Vegetation canopies assert a first order control on above-ground hydrological processes, therefore any hydrologic analysis of vegetation cover change must consider above-ground processes. In cold regions that receive some portion of precipitation as snow, the above-ground processes principally impacted are interception, throughfall, and snowpack dynamics, and hence timing and amount of surface water input (SWI). First, precipitation interception by vegetation canopies is a major component of the land surface water cycle, consisting of as much as half of the hydrological budget in some systems (Hörmann *et al.*, 1996; Carlyle-Moses, 2004). A large portion of intercepted precipitation is evaporated or sublimated to the atmosphere, defined here as interception loss, and therefore does not become throughfall and enter the soil profile (Calder, 1998). Second, in snow-dominated environments, vegetation cover can alter snowpack dynamics. This occurs both by reducing snow throughfall (Eddleman and Miller, 1991; Storck *et al.*, 2002), and altering snow surface energetics (e.g. net radiation and turbulent energy regimes) which affects snow deposition and snowmelt timing and amount (Golding and Swanson, 1978; Troendle and King, 1985; Ellis *et al*., 2013; Lundquist *et al.*, 2013). Both snow interception and accelerated snowmelt can produce tree wells – areas under tree canopies with less snow than open areas, which in addition to altered wind regimes, can cause snow to be redistributed under shrubs or trees compared to open or interspace areas (Robertson, 1947; Hutchison, 1965; Sturm *et al.*, 2001; Pomeroy *et al.*, 2006). A hydrological analysis of changes in vegetation cover must consider how interception, throughfall, and snowpack dynamics are impacted.

Understanding how precipitation phase (rain or snow) affects interception and throughfall dynamics is especially important since climate change is altering the fraction of precipitation that falls as snow in many regions. Research in the western U.S. shows shifts from snow to rain dominated precipitation regimes (Nayak *et al.*, 2010, Kapnick and Hall, 2012), which are likely to be even more drastic in the future (Klos *et al*., 2014). These shifts are associated with reduced streamflow (Luce and Holden, 2009; Berghuijs *et al*., 2014). Despite the importance of snow to streamflow in the western U.S. (Service, 2004), there is still a lack of a mechanistic understanding of the hydrological processes that drive these runoff reductions (Berghuijs *et al.*, 2014). A possible mechanistic link is changes in interception and throughfall dynamics. Intercepted rain is stored in the canopy for several minutes and up to a several days, and stemflow can consist of a small or large fraction of total rain throughfall (Eddleman and Miller, 1991; Crockford and Richardson, 2000; Levia, 2004; Carlyle-Moses and Price, 2006; Owens *et al*., 2006), although it is typically smaller in rough-barked trees common in semi-arid areas (Levia and Germer, 2015). On the other hand, intercepted snow can remain in the canopy from days to months (Storck *et al*., 2002; Parajka *et al.* 2012) and stemflow from melted snow is not typically observed or plays a minor role (Young *et al*., 1984; Eddleman and Miller, 1991; Levia, 2004).

Understanding how rain and snow interception and throughfall, as well as snowpack dynamics, differ is especially important in areas undergoing drastic land cover changes. Semi-arid tree-dominated woodlands, including western juniper and other pinyon-juniper dominated landscapes are currently the largest forest cover class in the western U.S. (Larson, 1980). This large spatial coverage is partly due to woodland encroachment into grass or shrub-dominated landscapes over the 140+ years that has seen increases by as much as 10-fold in pinyon-juniper coverage in some areas (Tausch *et al*., 1981; Miller *et al.*, 2005; Romme *et al.*, 2009). Assessing shifts from snow to rain interception and throughfall is especially important in western juniper (henceforth "juniper") areas since they principally occur at lower and mid-elevations (Gedney *et al.*, 1999) where the transition from snow to rain dominated regimes has and will likely continue to occur (Nayak *et al.*, 2010; Klos *et al.*, 2014). Land cover in these semi-arid systems will likely continue to shift due to juniper encroachment (Creutzburg *et al*., 2015) as well as large scale juniper removal by management agencies (Bureau of Land Management, 2015). Multiple studies have assessed interception loss in sagebrush spp. and juniper separately for both rain and snow with interception loss ranging from 44% to 55% in sagebrush (Collins, 1970) and 14% to 90% in juniper (Collings, 1966; Young *et al.*, 1984; Eddleman, 1986; Eddleman and Miller, 1991; Larsen, 1993; Taucer, 2006; Owens *et al.*, 2006). Throughfall in juniper can be greater in rain than in snow (Eddleman and Miller, 1991). Both sagebrush spp. and juniper can also alter snow redistribution dynamics, causing snow deposition on the leeward side of the vegetation structure (Tedesche, 2010). Despite the existence of these data, there is a paucity of studies directly comparing above-ground hydrological processes in juniper to sagebrush spp.

The impacts of both changes in vegetation and climate on above ground hydrological processes manifests itself through changes in SWI. While many studies focus on changes in snowpack from shifts in vegetation (Ellis *et al.*, 2013; Lundquist *et al.*, 2013) or shifts in climate (Mote *et al.*, 2005; Kapnick and Hall, 2012), ultimately the timing and amount of SWI exerts primary control on streamflow and ecosystem productivity in many environments (Seyfried *et al.*, 2009; Smith *et al.*, 2011). The timing of SWI is effectively synchronous with precipitation for rain events, but is asynchronous for snow events by hours or even months depending on the timing of snow melt. However, SWI amount may not directly correlate to snow deposition or peak snow water equivalent (SWE) due to snowpack sublimation (Reba *et al.*, 2012) or timing of SWI input (Seyfried *et al.*, 2009). Despite the importance of SWI, few studies focus on how both vegetation and climate shifts alter the timing and quantity of coupled interception, snowpack, and SWI dynamics.

The broad objective of this paper is to understand how shifts from snow to rain and changes in land cover alter above-ground interception, throughfall, snowpack, and SWI dynamics. Furthermore, the existence of western juniper woodlands in the snow-rain transition zones make it especially important to analyze how throughfall dynamics will change across both shifts in precipitation regime and land cover. To this end, the specific objectives of this paper are to (i) understand the differences between rain and snow throughfall in western juniper, (ii) understand how rain canopy storage and evaporation rates in western juniper are influenced by event-scale meteorological conditions, (iii) understand differences in snow accumulation, ablation, timing and amount of SWI, and evaporation and sublimation loss between western juniper, low sagebrush, and mountain big sagebrush.

METHODS

To assess the effects of climate and vegetation on above-ground hydrological fluxes, we used a combination of observations both to empirically compare processes and to validate a model to assess the effects of different climate and vegetation scenarios on hydrological fluxes.

Site Description

This study was conducted at the Reynolds Creek Experimental Watershed (RCEW) and Critical Zone Observatory (RCZO) in the Owyhee Mountains, approximately 80 km southwest of Boise, ID, USA. RCZO is a semi-arid watershed with moderate steepness and snow cover typically persisting for 4 to 6 months of the year. The specific site for this study is located at 1940 m above m.s.l. The slope and aspect of the study site are 26% and 246° respectively. Annual precipitation at the nearest gauge, located at a climate station 730 m to the east and 50 m higher in elevation from the study site, was 554 mm. Based on PRISM adjustment of monthly precipitation from the climate station (Daly *et al*., 1994), annual precipitation at the study site is estimated at 490 mm. Wind direction at the site is typically from the south by southwest, producing drifts on the north or northeast sides of topographic features (Winstral *et al*., 2009) or vegetation (Tedesche, 2010). Plant species on the site include a mix of western juniper (*Juniperus occidentalis*), low sagebrush (*Artemisia arbuscula*), and mountain big sagebrush (*Artemisia tridentata*). Equipment was established over an approximate two ha study area that included two areas with juniper: a savannah-like low density area with a canopy cover of 17% and in an adjacent medium density juniper area with a canopy cover of 37%.

Measurements

Meteorological data collected at a long-term climate station in the medium density juniper area includes air temperature (T_a), shortwave radiation, relative humidity, wind speed (*u*), wind direction, vapor pressure, and snow depth (D_S), all measured with standard methods (see Hanson 2001 for descriptions). Two trees (designated Tree 1 and Tree 2) were selected for intensive measurements. Tree 1 had a diameter (height) of 3.2 m (3.7 m) and Tree 2 had a diameter (height) of 2.7 m (2.8 m). Based on a vegetation survey, juniper trees at the study area had a median diameter of 2.9 m (n = 84), therefore Tree 1 and 2 are representative of the study area. Four large lysimeters, one at each tree and two in the interspace, were used to quantify rain, throughfall, and snowmelt. We constructed lysimeters out of plywood lined with an industrial tarp (see Elder et al. 2014 for a general schematic). The tree lysimeters were constructed to capture all throughfall under the canopy and the interspace lysimeters were a 2.4 x 2.4 m square. Water was funneled to an opening in a buried and insulated plywood box that contained a 250 ml tipping bucket. A volume of tip versus time rating curve was developed for each tipping bucket. Depth of rain, throughfall, and snowmelt were calculated based on the area of the lysimeter and volume of each tip. Freezing was an issue during the winter and we identified and removed erroneous data by comparing lysimeter data to precipitation, D_S, and modeled data. Although not continuous throughout the study period, the lysimeter events allowed for comparison of throughfall dynamics across discrete rain and snow events.

We collected continuous snow measurements by recording hourly digital images of snow stakes under and outside trees with the automated 6 megapixel Moultrie Game

Spy M-65. Since snow is most variable on north and south sides, we established two cameras pointed at Tree 1 (Tree 2) from the east (west) side. Snow stakes consisted of 1.5 m long, 1.3 – 3.8 cm diameter, PVC pipe with depth marks every 5 cm. Due to their small size, we assume these had little impact on snowmelt processes and therefore minimal impact on the lysimeter data During the first year, we placed two stakes under each tree – one on the north and south sides equidistance from the tree trunk and canopy edge. We also placed two snow stakes outside each tree, 0.5 m to 2.0 m from the canopy edge. During the second year, we placed six snow stakes under each tree, three located on both the north and south side of the tree positioned approximately 15 cm from the trunk, equidistance from the trunk and canopy edge, and approximately 15 cm from the canopy edge. Additionally, four stakes total were placed outside each tree in the interspace on the north and south sides and two on the camera side (east or west) of the tree. Digital photos, by establishing a pixel per cm depth, allowed for D_S measurement resolution of approximately 0.2 cm and manually estimation of D_S. We estimated D_S every hour during snow events and rapid ablation periods, and every 12 hours outside of those periods. Due to camera failure from Dec 5th, 2013 to Jan 30th, 2014, 74% of the active snow season (first snow fall to permanent snowpack melt) was captured.

We estimated rain interception loss (I_{rain}) for individual rain events based on the lysimeter measurements in the interspace (P_G) and under the tree (P_N). We calculated I_{rain} by:

$$I_{rain} = 1 - \frac{P_N}{P_G} \quad \textbf{[1]}$$

with P_G and P_N as the rain measured in the interspace and throughfall measured under the tree, respectively. P_G and P_N measurements were included from the start of the event to six hours after the rain event stopped to allow for canopy evaporation of intercepted rain.

We estimated the throughfall ratio (TF) both for rain and snow events with the following equation:

$$TF = \frac{P_N}{P_G} \textbf{ [2]}$$

where P_G was based on the average interspace storm snow accumulation or rain and/or snowmelt measured with the lysimeter. P_N was based on the rain and/or snowmelt measured with the lysimeter or storm snow accumulation under the tree at the particular snow stake (i.e. not averaged for the entire tree). First, we calculated rain TF (TF_{rain}) with lysimeter measurements under the tree and in the interspace. Second, we calculated TF with lysimeters for snow events with snow-free antecedent conditions ($TF_{snow,l}$) where the entire snowpack melted out before additional precipitation occurred, verified by the hourly photos. Third, we calculated mixed snow events TF (TF_{mixed}) where part of the event included snow but had some portion that occurred with T_a above 1°C. Fourth, snow TF ($TF_{snow,d}$) was estimated by comparing snow depth at snow stakes for snow events that occurred during the permanent snowpack. $TF_{snow,d}$ was calculated with the ratio of total under tree snowfall to interspace snowfall, both based on D_S measurements before and after the event. Note that in our calculation of $TF_{snow,d}$, P_N and P_G includes both snow that initially falls to the ground as well as deposited snow redistributed by wind. Although this constitutes two different processes, for simplicity we use $TF_{snow,d}$ to incorporate both. To compare TF_{rain} to both $TF_{snow.l}$ and TF_{mixed}, we calculated a P_G-

weighted average TF where an increasing weight on the portion of the event P_G to the total P_G.

We conducted several analyses to assess the metereological factors and that control both lysimeter-estimated TF (TF_{rain}, $TF_{snow,l}$, TF_{mixed}) and $TF_{snow,d}$. First, we developed two separate multiple linear regressions (MLR) for both lysimeter-estimated TF and $TF_{snow,d}$ with TF as the dependent variable and P_G (D_S outside the tree for $TF_{snow,d}$ MLR), average storm u and T_a, and tree type (Tree 1 or 2) as the independent variables, in addition to antecedent tree-interspace snow depth difference ($D_{tree\text{-}inter}$) for $TF_{snow,d}$ and VPD for lyimsiter-based TF. We performed a stepwise MLR that removed variables to lower the model Akaike Information Criteria (AIC) score (Burnham and Anderson, 2004). Second, we did a simple linear regression (SLR) between $TF_{snow,d}$ and $D_{tree\text{-}inter}$. To calculate how much additional snow is deposited under the trees due to $D_{tree\text{-}inter}$, we calculated $TF_{snow,d}$ without the influence of $D_{tree\text{-}inter}$ by using the SLR coefficients to remove the influence of $D_{tree\text{-}inter}$ on each $TF_{snow,d}$ estimate. For each storm we then averaged the added snow under the canopy across all snow stakes.

We conducted snow surveys to estimate the spatial variability of D_S across the site. We measured D_S along a 200 m north-south transect that crossed the low density and medium density juniper areas. We established a stratified random sampling design by collecting D_S every 10 m with two north/south or east/west offsets 4 m from each point, alternating the offset direction every other measurement. We measured D_S under adjacent trees by locating the closest tree from each initial point, and measuring D_S on the north and south sides at the trunk, between trunk and canopy edge, at the canopy edge, and 1 m outside the canopy edge. If no tree canopy was within a 10 m radius of the initial point, no tree D_S was measured. Our first survey on March 14th, 2013 was along four transects. We conducted snow surveys along one or two of the same initial transects in 2014 on Jan 30th, Feb 20th, and March 12th.

Canopy interception loss model

We estimated canopy storage capacity (S) and evaporation to rainfall rate during saturated canopy conditions ($\overline{E}/\overline{R}$) by comparing P_N and P_G. The Gash analytical model (Gash, 1979) estimates I_{rain} canopy parameters based on discrete events and has been successfully applied across a range of meteorological and vegetation characteristics (Gash and Morton, 1978; Lankreijer *et al*., 1993; Jetten, 1996; Schellekens *et al.*, 1999). The model combines mathematical representation of interception processes and an empirical approach based on measured P_G and P_N that span the canopy wetting and saturation period to derive S and $\bar{E}/\bar{R}$ (e.g. Link *et al.*, 2004). We estimated I_{rain} parameters for events with clear canopy saturation inflection points for both Tree 1 and 2.

To assess how I_{rain} parameters can change with meteorological characteristics of each storm, we plotted S and $\overline{E}/\overline{R}$ with P_G, VPD, and u. We also analyzed the relationship between $\overline{E}/\overline{R}$ and T_a. We plotted I_{rain} with time to understand seasonal dynamics. We plotted I_{rain} through time and not S, since there was a paucity of events that were large enough to estimate S. We used SLR and MLR to test the statistical significance of correlations between I_{rain} parameters and P_G, VPD, and u.

Simulation approach

To compare differences in above-ground hydrological fluxes under current and future climates and across juniper and sagebrush, we modeled hydrological fluxes with the Simultaneous Heat and Water (SHAW) model (Flerchinger *et al.*, 1996). SHAW is a one-dimensional model that simulates the water and energy fluxes within the soil-plant-atmosphere continuum at an hourly time scale. The model is driven by precipitation, shortwave radiation, *u*, T_a, and relative humidity. The SHAW model has been tested and applied extensively within low and mountain big sagebrush sites at RCZO (Flerchinger *et al*., 1996; Flerchinger *et al.*, 2010). To assess the sensitivity of hydrological fluxes to different vegetation cover characteristics we varied LAI, vegetation height, and albedo across juniper, mountain big sagebrush, and low sagebrush (Table 1). These and other parameter values were derived from previous SHAW studies (Flerchinger *et al*., 1996; Flerchinger *et al*., 2010; Chauvin *et al*., 2011) and empirical vegetation studies at RCZO (Clark and Seyfried, 2001).

We simulated the current and future hydrological fluxes with the SHAW model. Current simulations were run with meteorological data from the climate station at the site from 2007 to 2014 water year (WY) and precipitation data from PRISM-adjusted data from the uphill climate station (Daly *et al*., 1994). Future meteorological data was identical to the 2007 to 2014 WY data except T_a was changed. Future T_a was generated using projections from 20 global climate models (GCM) from the Multivariate Adaptive Constructed Analogs (MACA) data set (Abatzoglou and Brown, 2012). For the 8.5 representative concentration pathway for the 4 km or 6 km (GCM resolution varies) tile that overlaps with the study site, we calculated the change in monthly T_a from the current (1990-2005) and mid-century (2046-2065). This change in monthly T_a was then used to change each daily T_a measurement in WY 2007 – 2014. We assumed relative humidity would stay the same and the SHAW model calculates the changes in vapor pressure based on the input T_a and relative humidity. Although precipitation and other meteorological variables may change under future climates, we only modeled changes in T_a and corollary changes in vapor pressure because a) climate predictions show a clear shift in T_a (Hamlet and Lettenmaier, 2007; Abatzoglou and Brown, 2012) and b) precipitation predictions are less certain (Hamlet and Lettenmaier, 2007). The model does incorporate differences in the phase of precipitation with warming T_a, with precipitation being modeled as rain when T_a is above the snow T_a threshold (1 °C).

SHAW model performance was evaluated with the Nash-Sutcliffe model efficiency (Nash and Sutcliffe, 1970) by comparing A) daily simulated D_S in no vegetation with D_S at the climate station (WY 2007 to 2014), B) daily simulated D_S in juniper (no vegetation) with D_S under juniper canopy (interspace) averaged across representative snow stakes at trees 1 and 2, and C) weekly simulated SWI in juniper (no vegetation) with measured SWI at juniper (control) lysimeters. We validated SHAW with no vegetation since the climate station is kept bare and the interspace snow stakes and lysimeters are bare as well. We compared snowpack dynamics, SWI amount and timing, and evaporation/sublimation (ES) loss between the current and future simulations, as well as across the three vegetation types. We also calculated the day 50% of the total WY SWI has occurred (SWI 50% day). We used SLRs to compare the timing and amount of SWI to peak SWE.

RESULTS

Throughfall

A total of 11 snow events occurred with snow-free antecedent conditions where the entire snowpack melted before additional precipitation occurred, which allowed for estimation of $TF_{snow,l}$. P_G for these 11 events ranged from 1.1 mm to 13.0 mm (mean = 5.1 mm). The average $TF_{snow,l}$ for these events was 63.1% (n = 16, SD = 34.8%) (Figure 1) with two positive $TF_{snow,l}$ estimates. A positive estimated $TF_{snow,l}$ indicates a greater amount of snow deposited under the tree than in the open area. A total of four events included a portion of precipitation falling above and below 1.0 °C and were classified as "mixed". Average TF_{mixed} was 90.5% (n = 7, SD = 39.6%) (Figure 1). TF_{rain} was estimated at 25.1% (n = 29, SD=23.1%) (Figure 1). The average TF with snow ($TF_{snow,l}$ and TF_{mixed}) and TF_{rain}, weighted by P_G, was 79.4% and 54.8%, respectively. Comparing the current and future simulated climate, the total seasonal SWE to P_G ratio shifted from 63.6% to 37.3% (Figure 6). Calculating the total TF from these monthly precipitation shifts with the PG-weighted TF estimates, the total TF was 400 mm for 1990 – 2005 and 363 mm for 2046 – 2065, a 9.2% reduction from current to future TF.

Comparing $TF_{snow,l}$, TF_{mixed}, and TF_{rain}, both the storm type and P_G impacted estimated TF. For the MLR model with TF as the dependent variable, and the independent variables as T_a, u, VPD, P_G, tree type and storm phase, P_G ($p = 0.005$) and rainfall events ($p = 0.002$) were significant. Confirming our assumption of both trees as similar to each other, differences in TF between tree 1 and tree 2 were not significant ($p = 0.82$). A stepwise MLR of the same statistical model reduced the original six variables to VPD ($p = 0.07$), P_G ($p = 0.004$), as well as rain ($p = 0.0001$) and mixed ($p = 0.31$) event type. Furthermore, VPD, P_G, and storm phase explain 3.4%, 9.3%, and 17.0% of variation.

Event-based $TF_{snow,d}$ evidenced a relationship between $D_{tree\text{-}inter}$ and estimated $TF_{snow,d}$. $TF_{snow,d}$ increased for events that occurred for larger $D_{tree\text{-}inter}$ values (Figure 2). This relationship persisted regardless of P_G. Using SLR, the relationship between $TF_{snow,d}$ and $D_{tree\text{-}inter}$ was statistically significant (Figure 2, $p < 0.001$). Based on a one-way ANOVA, for the 34 snow storms during the second year, event D_S under the tree was statistically different at the snow stakes closest to the trunk compared to the middle and canopy edge snow stakes ($p = 0.03$), but the latter two were not statistically different ($p = 0.26$). The five term MLR was significant ($p < 0.0001$). The stepwise regression retained $D_{tree\text{-}inter}$ ($p = 0.001$), u ($p = 0.001$), T_a ($p = 0.11$) and tree type ($p = 0.11$), and P_G ($p = 0.15$).

Canopy Rain Interception Loss

A total of 29 rain events were captured with a P_G ranging from 0.31 mm to 21.1 mm (mean = 4.9 mm). The average event-based I_{rain} for both trees was 74.9% (n = 52, standard deviation (SD) = 23%) (Figure 1). For the 18 (34) rain events larger (smaller) than 5 mm, the average I_{rain} was 48.7% (84.0%,). Plots of the 11 rainfall events large enough to model S indicate clear inflection points in plots of P_G vs. P_N and allowed for I_{rain} parameters to be determined for both trees (i.e. n = 22). These storms averaged 9.3 mm. The average S was 2.0 mm and there was not a statistically significant relationship between P_G (Figure 3a) or u (Figure 3b) , although u was statistically significant in the MLR ($p = 0.02$). The relationship between VPD and S was significant (Figure 3c). There was an I_{rain} seasonal pattern with maximum I_{rain} during the middle-growing season months of May to September, and lower I_{rain} in the beginning and end of the growing season (Figure 4). In addition, P_G also correlated with I_{rain} (Figure 4).

Estimated $\overline{E}/\overline{R}$ during rain events was correlated principally with P_G (Figure 3d), which was statistically significant in predicting $\overline{E}/\overline{R}$ in the MLRs ($p < 0.0001$). There was no clear correlation between $\overline{E}/\overline{R}$ and both *u* (Figure 3e) and VPD (Figure 3f). However, correlation between $\overline{E}/\overline{R}$ and both *u* and VPD is greater when only considering events larger than 10 mm (Figure 3e,f). T_a is also positively correlated with $\overline{E}/\overline{R}$ (regression not displayed: slope = 0.01 mm hr^{-1} $°C^{-1}$, $p = 0.06$).

Snow Deposition

$TF_{snow,d}$ was estimated from 65 snow events that occurred as early as September 26th and as late as April 27th. A total of 261 below-tree D_S measurements occurred since each tree had anywhere from two to six snow stakes under the canopy. Total D_S accumulation per snow event outside the tree ranged from 0.7 cm to 30 cm and averaged 5.3 cm. Average event $TF_{snow,d}$ ranged from 0% to 171% with an average of 58.5% (SD = 33.1%) (Figure 1). The largest measured winter event during the study period was 30 cm D_S, but snow on the tree branches obscured snow stakes under the trees preventing a below-tree D_S estimate. The largest event where D_S under the trees could be identified was 12 cm D_S and the TF was 49% at the south canopy edge stake and 45% at the north middle canopy stake. Calculated snow deposition due to $D_{tree\text{-}inter}$ was 15.2 cm and 13.9 cm for WY 2013 and WY 2014 respectively, and the complete WY 2014 snow season was not recorded (Figure 5).

Snowpack Dynamics

Snow surveys across the plot in the interspace and under the trees show that in general the continuous measurements were representative of the two ha study area (Figure 5). These continuous measurements reveal that snowpack dynamics under the tree and in the interspace comprised almost entirely different snowpack ablation and melt regimes. In WY 2013, under the tree D_S was often less than 5 cm or entirely absent starting in mid-January (Figure 5A). Conversely, average D_S in the interspace was persistently deeper and not less than 25 cm until the majority of the snowpack ablation occurred mid-March (Figure 5A). In WY 2014, on January 30th snowpack under the tree was absent for six of the eight snow stakes and the interspace average D_S was 9.7 cm (Figure 5B). That same year after a large snow event in early February, the snow under trees disappeared almost entirely again before another snow event in late February (Figure 5B). Conversely, snow persisted in the interspace through several snow events in late February before disappearing from all the interspace stakes by March 3rd and March 9th (Figure 5B).

Current and Future Simulations

The Nash-Sutcliffe model efficiency comparing measured D_S at the climate station, D_S in the interspace, and D_S under the juniper canopy with simulated D_S was 0.78, 0.81, and 0.51. Model efficiency for SWI at lysimeters under the two trees was -0.01 and 0.37 respectively, and in the interspace lysimeters were 0.41 and 0.49 respectively. The average monthly T_a increase between the current and mid-century simulations ranged from 2.2 to 3.2 °C, with January, July, August, and September all above 3 °C. As a result, monthly ratios of simulated SWE to P_G show a clear shift to less snow under a future climate (Figure 6). The average snowfall to P_G ratio from December to March ranged from 0.84 to 0.89 in the current climate, and shifted to 0.47 to 0.57 in the mid-21st century climate (Figure 6).

Modeled SWE in juniper compared to the two sagebrush simulations is consistently lower throughout the winter (Figure 7). The average peak SWE for the current climate in juniper is 153 mm, compared to 236 mm and 222 mm for mountain and low sagebrush respectively. Juniper therefore have 31% and 35% lower peak SWE than mountain and low sagebrush respectively. This difference in peak SWE between juniper and low sagebrush of 83 mm is 17% of the total annual water budget. Under future simulations, average juniper peak SWE was 46 mm, compared to 67 mm and 74 mm under mountain and low sagebrush respectively. Juniper reduce peak SWE by 30% and a 37% compared to mountain and low sagebrush respectively (Figure 7). Average snow cover disappearance for the three species were within 2 days of each other for the current climate, and within 12 days of each other for the future climate, with snow disappearance occurring earliest in juniper in both cases (Table 2). However, snow disappearance day from the current to future simulations shifted on average 51 days across the three vegetation types (Table 2).

Shifts in climate and vegetation both produced differences in timing and quantity of SWI. SWI was greater in both low and mountain big sagebrush, compared to juniper, in both the future and current simulations by an average of 137 mm (Table 2). In general, SWI shifted to earlier in the season, with Winter (Nov – Feb) SWI greater in future climate compared to current climate across all vegetation types. Under the current climate, SWI peaked in April, especially in low and mountain big sagebrush (Figure 8 A-C) which both had deeper peak SWE compared to juniper (Figure 7). These April peaks in SWI in the current simulations for juniper, mountain big sagebrush, and low sagebrush were respectively 34 mm, 104 mm, and 104 mm greater than the March – the next largest SWI month for each simulation. Conversely, average SWI peaked in March in the future climate, which were 19 mm, 44 mm, 56 mm greater than January, the next greatest average SWI month in each simulation. These future March SWI peaks were 38%, 44%, and 41% lower than the current April SWI peaks in juniper, mountain big sagebrush, and low sagebrush respectively. These shifts in SWI are reflected in the SWI 50% day which shifted to an average of 45 days earlier across the three vegetation types (Table 2).

By comparing peak SWE to both the amount and timing of SWI, we see how a warmer climate impacts SWI timing and quantity. Peak SWE correlates with SWI amount for years when Nov – Mar T_a is on average below 0 °C (Figure 9A). But peak SWE is not similarly correlated with SWI when average Nov – Mar T_a is above 0 °C (Figure 9A). Conversely, the timing of SWI correlates with peak SWE (Figure 9B) regardless of T_a as both cold and warm years fall along the same trend. 50% SWI occurs earlier in years that are both warmer and with lower peak SWE.

Combined ES loss principally differs in the amount across juniper and the sagebrush species and in timing across both simulations. ES loss was on average 92 mm greater in the juniper compared to the two sagebrush simulations, but only 19.7 mm greater in the future juniper simulation compared to the current juniper simulation (Table 2). In general, from the current to future simulations, ES shifted earlier with increases in February, March, and April and little or no changes occurred in June through November (Figure 8D-F). In the juniper simulations, ES loss peaked in June in the current simulation, but peaked in March in the future simulation (Figure 8D). Conversely, in mountain and low sagebrush although ES loss increased in November through June between the current and future simulations, the peak monthly ES loss was in June or July (Figure 8E,F). Clearly changes in the climate shift the timing of ES, but differences in vegetation primarily shift the amount of ES.

DISCUSSION

I_{rain} and S in juniper were within the range of previous estimates. Our median I_{rain} of 74.9% is similar to other western juniper and similar semi-arid tree species studies that range from 29% to 71% (Young *et al.*, 1984; Eddleman, 1986; Eddleman and Miller, 1991; Larsen, 1993). Our estimate is probably on the upper end of the I_{rain} range because most of the rain events are small (mean = 4.9 mm). Finally, our average S of 2.0 mm was vey similar to Larsen's (1993) average of 1.9 mm, who used simulated rain at 23 mm hr^{-1} for juniper ranging from 2.5 to 10.4 m in diameter.

Our analysis pointed to clear differences in TF due to both precipitation type and P_G. We observed differing TF estimates for TF_{rain} and $TF_{snow,l}$ of 54.8% and 79.4% respectively. The TF group mean for both rain and mixed events in the MLR were statistically different being lower and higher than the overall mean respectively. Conversely, Eddleman and Miller (1991) observed greater TF_{rain} of 48.0% compared to $TF_{snow,l}$ of 39.6%. P_G was also statistically significant in our MLR with increasing P_G corresponding to increasing TF. The fact that P_G was statistically significant is important in the fact that future models predict greater winter P_G (Kumar *et al.*, 2012), which would potentially increase TF and thereby offset the decreases in TF due to shifts from snow to rain. Interestingly, in Eddleman and Miller's study of the average P_G was much larger for snow (53 mm) than rain (8.3 mm), despite a lower observed $TF_{snow,l}$ compared to TF_{rain}. A possible reason for differences in the effect of P_G across $TF_{snow,l}$ and TF_{rain} is u. Eddleman and Miller surmised that high $TF_{snow,l}$ is due to the lack of wind which allowed for intercepted snow to remain in the canopy for longer time periods to ultimately be sublimated, reducing total $TF_{snow,l}$. Our study supports the potential for wind increasing

TF with u being significant in the $TF_{snow,d}$ MLR, however it was not significant in the lysimeter-based MLR.

In addition to both precipitation type and P_G driving TF, increases in VPD also alters TF dynamics. First, post-event VPD was correlated with decreasing TF across event type, and was retained in the stepwise MLR. Likewise, for our I_{rain} parameter analysis, $\overline{E}/\overline{R}$ was correlated with increasing T_a and VPD. VPD is driven in part by T_a, therefore increases in T_a are likely to produce increases in VPD. With the $\overline{E}/\overline{R}$ vs. T_a regression slope of 0.01 mm hr^{-1} °C^{-1}, a 5 °C warming would increase $\overline{E}/\overline{R}$ by 0.05 mm, increasing I_{rain} an additional 1 mm for a a 20 hour storm.

While TF_{rain} and $TF_{snow,l}$ differed, differences in $TF_{snow,d}$ and interspace-canopy snowpack dynamics were apparent. Differences in D_S between the tree and interspace persisted throughout the winter (Figure 5). $TF_{snow,d}$ increased for events that were a) windier and b) had greater difference in $D_{tree\text{-}inter}$. We estimated an additional 15.2 cm and 13.9 cm each year was deposited under the canopy due to $D_{tree\text{-}inter}$. This produces a counter-intuitive snowpack dynamic where there can be less snow under the tree but a greater amount of snow can be deposited under the tree than the interspace (Figure 2). Similar to other tree and shrub studies in cold environments, tree wells often form under trees due to canopy interception and emission of longwave radiation from tree boles (Robertson, 1947; Hutchison, 1965; Sturm *et al.*, 2001; Pomeroy *et al.*, 2006). Other shrub studies have also observed increased under-canopy snow deposition within these wells around shrubs (Hutchison, 1965; Essery and Pomeroy, 2004; Pomeroy *et al.*, 2006; Tedesche, 2010). Our study is a first step in revealing that there are similar dynamics in juniper. These increases in snow deposition below a tree could potentially provide a soil moisture subsidy that increases localized soil moisture, similar to snow drifting on leeward sides of topographic features (Seyfried *et al.*, 2009). It is also likely that snow energetics plays a primary role in below canopy snow melt and subsequent tree well formation. Future studies could further elucidate the role of snow energetics in snowpack dynamics in juniper and how they differ between juniper and sagebrush.

I_{rain} showed seasonal dynamics with peak I_{rain} in the middle of the summer. There are several possible reasons for this seasonal pattern. First, it is likely due in part to the P_G. Larger events occurred in the late spring and early fall, and P_G is inversely correlated with I_{rain} (Figure 1). Second, VPD increased estimated $\bar{E}/\bar{R}$ (Figure 2F), and higher VPD is observed in the middle of the summer compared to the beginning and end of the growing season. Third, juniper bud elongation occurs in early spring and their needles die in the fall (Miller *et al.*, 2005). However, the dead needles often do not fall immediately, but can stay attached to the tree for several years (Miller, *personal communication*). Link *et al.* (2004) found that in Douglas fir, there was a clear seasonal component of S linked with bud elongation and needle drop. Future studies could further clarify if this relationship holds in juniper, or if VPD and P_G exerts a stronger control on interception than juniper seasonal needle changes.

Simulations revealed that projected future increases in T_a primarily drive shifts in the timing rather than amount of hydrological fluxes. First, both snow disappearance day and SWI 50% day were 41 to 56 days earlier between the current and future simulations, with little change in the amount of SWI (Table 2). Similarly, ES loss shifted to earlier in the season between current and future climate simulations (Figure 8D-F). These shifts to more winter-dominated SWI are congruent a greater portion of winter precipitation occurring as rain in our simulations (Figure 6) and Klos *et al.* (2014). The similarity in the snow disappearance and SWI shifts are confirmed by other studies where snow disappearance corresponds to both peak soil moisture and peak runoff (Molotch *et al.*, 2009; Seyfried *et al.*, 2009; Smith *et al.*, 2011). Furthermore, our findings confirm other large scale studies in the western U.S. for both the last century (Regonda *et al.*, 2005) and future simulations (Elsner *et al.*, 2010), which show that with warming T_a total annual discharge was not greatly reduced but peak streamflow shifting to earlier in the winter.

Contrary to shifts in climate, shifts in vegetation primarily drive shifts in the quantity of hydrological fluxes. Simulated SWI for both the current and future simulations was on average 137 mm greater in both sagebrush species than in juniper (Table 2). Only one previous study we are aware of compares open area and forested SWI, and although in a mature conifer forests in humid western Washington state, it shows the same general increase in open area compared to under-canopy SWI (Harr *et al.*, 1989). Finally, ES loss is on average 92 mm higher in juniper than in both sagebrush species (Table 2). These similar shifts in SWI and ES loss are linked via interception and throughfall processes. Juniper LAI of 3.0 is greater than LAI in mountain and low sagebrush of 0.9 and 0.3 respectively. This higher LAI corresponds directly to higher S in the model, increasing the amount of intercepted rain and snow lost to the atmosphere and reducing the amount of throughfall reaching the soil. This equates to greater ES loss (Figure 8D) and reduced SWI (Figure 8A).

One exception to hydrological fluxes shifting in timing across the future and current simulations and in amount across the different vegetation simulations is peak SWE, which shifted both with changes in climate and vegetation. Across the three vegetation scenarios, the average peak SWE from the current to future simulations decreased on average 57.8%. This finding is confirmed by many measured (Mote *et al.*, 2005; Regonda *et al.*, 2005; Kapnick and Hall, 2012) and future simulations (Elsner *et al.*, 2010). Peak SWE was also much lower in juniper than in the two sagebrush simulations for the future and current simulations (Figure 7). This reduced peak SWE in juniper is due to increased interception and elevated below canopy radiation that increases snowmelt and thereby losses of water from snowpack. This greater loss of SWE under the canopy is confirmed with the lysimeter data, which although not continuous throughout both winters, when they were operational in the winter often had almost double SWI in the canopy than the interspace. Other studies comparing tree and interspace or small shrub-dominated open areas, although in large conifer systems, similarly show lower peak SWE outside of the tree canopy (Golding and Swanson, 1978; Troendle and King, 1985; Ellis *et al.*, 2013; Lundquist *et al.*, 2013).

Above-ground vegetation and climate change studies often focus on changes in peak SWE (Mote *et al.*, 2005; Regonda *et al.*, 2005; Kumar *et al.*, 2012; Lundquist *et al.*, 2013). While these are good first initial steps, these studies did not assess SWI, which does not necessarily correlate directly to SWE since snow deposition (Figure 2) and sublimation rates (Reba *et al.*, 2012) can vary between open and under canopy areas. Our study revealed that although peak SWE timing corresponds to timing of SWI (Figure 9B), it does not predict total SWI (Figure 9A). SWI is a key link between above-ground processes and streamflow generation (Seyfried *et al.*, 2009), and as climate shifts from snow to rain-dominated precipitation and winter SWI increases, it will be important to consider not only change in SWE, but changes in the timing and amount of SWI.

Finally, our study does not reveal a clear mechanism for why greater water yield has been observed during snow dominated compared to rain dominated years (Berghuijs *et al.*, 2014). Although $TF_{snow,l}$ was greater than TF_{rain} and both were significantly different in the MLR, wind also increased $TF_{snow,l}$. Furthermore, in comparing the future and current simulations, reductions in ES loss only changed slightly between current and future simulations (Table 2). In contras, differences in vegetation cover had a much greater impact on ES loss (Table 2). Further studies could elucidate the mechanism for observed differences in runoff.

CONCLUSIONS

There are clear differences in above-ground hydrological fluxes between juniper and sagebrush species. Average $TF_{snow,l}$ was 79.4% in juniper compared to TF_{rain} of 54.8%. TF and I_{rain} were both driven by P_G, with increasing P_G increasing TF and decreasing I_{rain}. T_a and VPD also altered above-ground processes, increasing post-storm VPD decreased TF and increased I_{rain}, and increasing T_a increased $\overline{E}/\overline{R}$. This has implications for how warming T_a could alter interception dynamics. Snowpack accumulation and ablation regimes were significantly different in the interspace dominated by low sagebrush than under juniper, with snow persisting 13 days longer in the interspace than under the trees and snow being more transient under the tree. It is therefore likely that increases in juniper cover will decrease late season snowpack that produces the delayed release of snowmelt that is key to support regional streams. Also, shifts from juniper to sagebrush will potentially decrease SWI by 137 mm, which is 24% of the total water budget.

Dramatic shifts in climate have occurred in many semi-arid systems and will likely continue to occur into the future. Our simulations revealed that warming over the next 40 years could cause the snowpack to disappear 51 days earlier and SWI, a major determinant of peak streamflow, to occur 45 days earlier. Land managers choices for future juniper management activities will therefore directly impact the hydrological fluxes in these semi-arid systems.

ACKNOWLEDGEMENTS

The authors wish to thank Steve Van Vactor, Mark Murdock, Ben Soderquist, and Jim Hoppie for their help with fieldwork. We thank the Reynolds Creek CZO NSF (EAR 1331872) for their field and data support. This work was funded by the National Science Foundation's IGERT (Award 0903479) and CBET (Award 0854553) programs, and the United States Geological Survey's Northwest Climate Science Center Doctoral Fellowship.

CITATIONS

Abatzoglou, JT, Brown, TJ. 2012. A comparison of statistical downscaling methods suited for wildfire applications. *International Journal of Climatology* **32**: 772-780. DOI:10.1002/joc.2312.

Berghuijs, WR, Woods, RA, Hrachowitz, M. 2014. A precipitation shift from snow towards rain leads to a decrease in streamflow. *Nature Climate Change* **4**: 1-4. DOI:10.1038/NCLIMATE2246.

Bureau of Land Management. 2015. Notice of Intent To Prepare an Environmental Impact Statement for the Proposed Bruneau-Owyhee SageGrouse Habitat Project, Owyhee County, Idaho. 12. Federal Register 2015-00741, 2725-2726, Washington, DC, USA.

Burnham, KP, Anderson, DR. 2004. Multimodel inference understanding AIC and BIC in model selection. *Sociological methods & research* **33**: 261-304.

Calder, I.R. 1998. Water use by forests, limits and controls. *Tree Physiology* **18**: 625-631.

Carlyle-Moses, D. 2004. Throughfall, stemflow, and canopy interception loss fluxes in a semi-arid Sierra Madre Oriental matorral community. *Journal of Arid Environments* **58**: 181-202. DOI:10.1016/S0140-1963(03)00125-3.

Carlyle-Moses, DE, Price, AG. 2006. Growing-season stemflow production within a deciduous forest of southern Ontario. *Hydrological Processes* **20**: 3651-3663. DOI:10.1002/hyp.6380.

Chauvin, GM, Flerchinger, GN, Link, TE, Marks, D, Winstral, AH, Seyfried, MS. 2011. Long-term water balance and conceptual model of a semi-arid mountainous catchment. *Journal of Hydrology* **400**: 133-143. DOI:10.1016/j.jhydrol.2011.01.031.

Clark, PE, Seyfried, MS. 2001. Point sampling for leaf area index in sagebrush steppe communities. *Journal of range management* **54**: 589-594.

Collings, M.R. 1966. *Throughfall for Summer Thunderstorms in a Juniper and Pinyon Woodland, Cibecue Ridge, Arizona*. U.S. Geological Survey Professional Paper 485-B.

Collins, DD. 1970. Climate-plant relations affecting semi-desert grassland hydrology. In *Simulation and Analysis of Dynamics of a Semi-desert Grassland, Range Science Department vol 6, 100-118, Colorado State University, Fort Collins, Colorado, USA.*

Creutzburg, MK., Henderson, EB, Conklin, DR. 2015. Climate change and land management impact rangeland condition and sage-grouse habitat in southeastern

Oregon. *AIMS Environmental Science* **2**: 203-236. DOI:10.3934/environsci.2015.2.203.

Crockford, RH, Richardson, DP. 2000. Partitioning of rainfall into throughfall, stemflow and interception: effect of forest type, ground cover and climate. *Hydrological processes* **14**: 2903-2920. DOI:10.1002/1099-1085(200011/12)14:16/17<2903::AID-HYP126>3.0.CO;2-6.

Daly, C, Neilson, RP, Phillips, DL. 1994. A statistical-topographic model for mapping climatological precipitation over mountainous terrain. *Journal of applied meteorology* **33**: 140-158.

Eddleman, LE. 1986. Canopy Interception of Precipitation. In, *Water Resources Research Institute, Oregon State University, Corvallis, Oregon, USA.*

Eddleman, LE, Miller, PM. 1991. Potential impacts of western juniper on the hydrologic cycle. In *Proceedings, symposium in ecology and management of riparian shrub communities, 176-180, Sun Valley, ID, USA, 29-31 May 1991.* Intermountain Research Station, US Forest Service. Ogden Utah, USA.

Elder, K, Marshall, HP, Elder, L, Starr, B, Karlson, A, Robertson, J. 2014. Design and Installation of a Tipping Bucket Snow Lysimeter. In *Proceedings, International Snow Science Workshop, 816–824, Banff, California, USA.*

Ellis, CR, Pomeroy, JW, Link, TE. 2013. Modeling increases in snowmelt yield and desynchronization resulting from forest gap-thinning treatments in a northern mountain headwater basin. *Water Resources Research* **49**: 936-949. DOI:10.1002/wrcr.20089.

Elsner, MM, Cuo, L, Voisin, N, Deems, JS, Hamlet, AF, Vano, JA, Mickelson, KE, Lee, SY, Lettenmaier, DP. 2010. Implications of 21st century climate change for the hydrology of Washington State. *Climatic Change* **102**: 225-260. DOI:10.1007/s10584-010-9855-0.

Essery, R, Pomeroy, JW. 2004. Vegetation and Topographic Control of Wind-Blown Snow Distributions in Distributed and Aggregated Simulations for an Arctic Tundra Basin. *Journal of Hydrometeorology* **5**: 735-744.

Flerchinger, GN, Hanson, CL, Wight, JR. 1996. Modeling evapotranspiration and surface energy budgets across a watershed. *Water Resources Research* **32**: 2539-2548. DOI:10.1029/96WR01240.

Flerchinger, GN, Marks, D, Reba, ML, Yu, Q, Seyfried, MS. 2010. Surface fluxes and water balance of spatially varying vegetation within a small mountainous headwater catchment. *Hydrology & Earth System Sciences* **14**: 965-978. DOI:10.5194/hess-14-965-2010.

Gash, JHC. 1979. An analytical model of rainfall interception by forests. *Quarterly Journal of the Royal Meteorological Society* **105**: 43-55.

Gash, JHC, Morton, AJ. 1978. An application of the Rutter model to the estimation of the interception loss from Thetford forest. *Journal of Hydrology* **38**: 49-58. DOI:10.1016/0022-1694(78)90131-2.

Gedney, DR, Azuma, D, Bolsinger, C, McKay, N. 1999. *Western Juniper in Eastern Oregon*. General Technical Report PNW-GTR-464, 64pp. US Department of Agriculture, Forest Service, Pacific Northwest Research Station, Portland, Oregon, USA.

Golding, DL, Swanson, RH. 1978. Snow accumulation and melt in small forest openings in Alberta. *Canadian Journal of Forest Research* **8**: 380-388.

Hamlet, AF, Lettenmaier, DP. 2007. Effects of 20th century warming and climate variability on flood risk in the western U.S. *Water Resources Research* **43**: W06427. DOI:10.1029/2006WR005099.

Harr, D, Coffin, B, Cundy, T. 1989. *Effects of timber harvest on rain-on-snow runoff in the transient snow zone of the Washington Cascades.* Interim Technical Report TFW-l8A-89-003, 30pp. United States Forest Service, Pacific Northwest Forest and Range Experiment Station. Portland, Oregon, USA.

Hörmann, G, Branding, A, Clemen, T, Herbst, M, Hinrichs, A, Thamm, F. 1996. Calculation and simulation of wind controlled canopy interception of a beech forest in Northern Germany. *Agricultural and Forest Meteorology* **79**: 131-148. DOI:10.1016/0168-1923(95)02275-9.

Hutchison, BA. 1965. S*now Accumulation and Disappearance Influenced by Big Sagebrush.* Research Note RM-46, 8pp. United States Forest Service, Rocky Mountain Forest and Range Station, Fort Collins, Colorado, USA.

Jetten, VG. 1996. Interception of tropical rain forest: performance of a canopy water balance model. *Hydrological Processes* **10**: 671-685. DOI: 10.1002/(SICI)1099-1085(199605)10:5<671::AID-HYP310>3.0.CO;2-A.

Kapnick, S, Hall, A. 2012. Causes of recent changes in western North American snowpack. *Climate dynamics* **38**: 1885-1899. DOI:10.1007/s00382-011-1089-y.

Klos, PZ, Link, TE, Abatzoglou, JT. 2014. Extent of the rain-snow transition zone in the western US under historic and projected climate. *Geophysical Research Letters* **41**: 4560-4568. DOI: 10.1002/2014GL060500.

Kumar, M, Wang, R, Link, TE. 2012. Effects of more extreme precipitation regimes on maximum seasonal snow water equivalent. *Geophysical Research Letters*, **39**: L20504. DOI:10.1029/2012GL052972.

Lankreijer, H, Hendriks, MJ, Klaassen, W. 1993. A comparison of models simulating rainfall interception of forests. *Agricultural and Forest Meteorology* **64**: 187-199. DOI:10.1016/0168-1923(93)90028-G.

Larsen, RE. 1993. *Interception and Water Holding Capacity of Western Juniper*. Thesis, Oregon State University, Corvallis, Oregon, USA.

Larson, FR. 1980. Pinyon-Juniper. In *Forest cover types of the United States and Canada.* Eyre, FH (ed). Society of American Foresters: Washington, DC, USA; 116-117.

Levia, DF. 2004. Differential winter stemflow generation under contrasting storm conditions in a southern New England broad-leaved deciduous forest. *Hydrological Processes* **18**: 1105-1112. DOI:10.1002/hyp.5512.

Levia, DF, Germer, S. 2015. A review of stemflow generation dynamics and stemflow-environment interactions in forests and shrublands. *Reviews of Geophysics*. DOI:10.1002/2015RG000479.

Link, TE, Unsworth, M, Marks, D. 2004. The dynamics of rainfall interception by a seasonal temperate rainforest. *Agricultural and Forest Meteorology*: **124** 171-191. DOI:10.1016/j.agrformet.2004.01.010.

Luce, CH, Holden, ZA. 2009. Declining annual streamflow distributions in the Pacific Northwest United States, 1948–2006. *Geophysical Research Letters* **36**: DOI:10.1029/2009GL039407.

Lundquist, JD, Dickerson-Lange, SE, Lutz, JA, Cristea, NC. 2013. Lower forest density enhances snow retention in regions with warmer winters: A global framework developed from plot-scale observations and modeling. *Water Resources Research* **49**: 6356-6370. DOI:10.1002/wrcr.20504.

Miller, RF, Bates, JD, Svejcar, TJ, Pierson, FB, Eddleman, LE. 2005. Biology, ecology, and management of western juniper (*Juniperus occidentalis*). Technical Bulletin 152, 82pp. Oregon State University, Agricultural Experiment Station, Corvallis, Oregon, USA.

Molotch, NP, Brooks, PD, Burns, SP, Litvak, M, Monson, RK, McConnell, JR, Musselman, K. 2009. Ecohydrological controls on snowmelt partitioning in mixed-conifer sub-alpine forests. *Ecohydrology* **2**: 129-142. DOI:10.1002/eco.48.

Mote, PW, Hamlet, AF, Clark, MP, Lettenmaier, DP. 2005. Declining mountain snowpack in western North America. *Bulletin of the American Meteorological Society* **86**: 39-49. DOI:10.1175/BAMS-86-1-39.

Nash, J, Sutcliffe, JV. 1970. River flow forecasting through conceptual models part I-A discussion of principles. *Journal of hydrology* **10**: 282-290.

Nayak, A, Marks, D, Chandler, DG, Seyfried, MS. 2010. Long-term snow, climate, and streamflow trends at the Reynolds Creek Experimental Watershed, Owyhee Mountains, Idaho, United States. *Water Resources Research* **46**: W06519. DOI:10.1029/2008wr007525.

Owens, MK, Lyons, RK, Alejandro, CL. 2006. Rainfall partitioning within semiarid juniper communities: effects of event size and canopy cover. *Hydrological Processes* **20**: 3179-3189. DOI:10.1002/hyp.6326.

Parajka, J, Haas, P, Kirnbauer, R, Jansa, J, Blöschl, G. 2012. Potential of time-lapse photography of snow for hydrological purposes at the small catchment scale. *Hydrological Processes* **26**: 3327-3337. DOI:10.1002/hyp.8389.

Pomeroy, JW, Bewley, DS, Essery, R, Hedstrom, NR, Link, TE, Granger, RJ, Sicart, JE, Ellis, CR, Janowicz, JR. 2006. Shrub tundra snowmelt. *Hydrological Processes* **20**: 923-941. DOI:10.1002/hyp.6124.

Reba, ML, Pomeroy, J, Marks, D, Link, TE. 2012. Estimating surface sublimation losses from snowpacks in a mountain catchment using eddy covariance and turbulent transfer calculations. *Hydrological Processes* **26**: 3699-3711. DOI:10.1002/hyp.8372.

Regonda, SK, Rajagopalan, B, Clark, M, Pitlick, J. 2005. Seasonal Cycle Shifts in Hydroclimatology over the Western United States. *Journal of Climate* **18**: 372-384. DOI:10.1175/JCLI-3272.1.

Robertson, JH. 1947. Responses of Range Grasses to Different Intensities of Competition with Sagebrush (*Artemisia Tridentata Nut*t.). *Ecology*, **28**:1-16.

Romme, WH, Allen, CD, Bailey, JD, Baker, WL, Bestelmeyer, BT, Brown, PM, Eisenhart, KS, Floyd, ML, Huffman, DW, Jacobs, BF, Miller, RF, Muldavin, EH, Swetnam, TW, Tausch, RJ, Weisberg, PJ. 2009. Historical and modern disturbance regimes, stand structures, and landscape dynamics in pinon-juniper vegetation of the western United States. *Rangeland Ecology & Management* **62**: 203-222. DOI:10.2111/08-188R1.1.

Schellekens, J, Scatena, FN, Bruijnzeel, LA, Wickel, AJ. 1999. Modelling rainfall interception by a lowland tropical rain forest in northeastern Puerto Rico. *Journal of Hydrology* **225**: 168-184. DOI:10.1016/S0022-1694(99)00157-2.

Service, R.F. 2004. Water resources: As the west goes dry. *Science* **303**: 1124-1127.

Seyfried, MS, Grant, LE, Marks, D, Winstral, A, McNamara, J. 2009. Simulated soil water storage effects on streamflow generation in a mountainous snowmelt environment, Idaho, USA. *Hydrological processes* **23**: 858-873. DOI: 10.1002/hyp.7211.

Smith, TJ, McNamara, JP, Flores, AN, Gribb, MM, Aishlin, PS, Benner, SG. 2011. Small soil storage capacity limits benefit of winter snowpack to upland vegetation. *Hydrological Processes* **25**: 3858-3865. DOI:10.1002/hyp.8340.

Storck, P, Lettenmaier, DP, Bolton, SM. 2002. Measurement of snow interception and canopy effects on snow accumulation and melt in a mountainous maritime climate, Oregon, United States. *Water Resources Research* **38**: 1-16. DOI:10.1029/2002WR001281.

Sturm, M, Holmgren, J, McFadden, JP, Liston, GE, Chapin III, FS, Racine, CH. 2001. Snow-shrub interactions in Arctic tundra: a hypothesis with climatic implications. *Journal of Climate* **14**: 336-344. DOI: 10.1175/1520-0442(2001)014<0336:SSIIAT>2.0.CO;2.

Taucer, PI. 2006. The Effects of Juniper Removal on Rainfall Partitioning in the Edwards Aquifer Region: Large-Scale Rainfall Simulation Experiments. Thesis, Texas A&M University, College Station, Texas, USA.

Tausch, RJ, West, NE, Nabi, AA. 1981. Tree age and dominance patterns in Great Basin pinyon-juniper woodlands. *Journal of Range Management* **34**: 259-264. DOI:10.2307/3897846.

Tedesche, ME. 2010. *Snow Depth Variability in Sagebrush Drifts in High Altitude Rangelands, North Park, Colorado*. Thesis, Colorado State University, Fort Collins, Colorado, USA.

Troendle, CA, King, RM. 1985. The effect of timber harvest on the Fool Creek watershed, 30 years later. *Water Resources Research* **21**: 1915-1922. DOI:10.1029/WR021i012p01915.

Winstral, A, Marks, D, Gurney, R. 2009. An efficient method for distributing wind speeds over heterogeneous terrain. *Hydrological processes* **23**: 2526-2535. DOI:10.1002/hyp.7141.

Young, JA, Evans, RA, Easi, DA. 1984. Stem flow on western juniper (*Juniperus occidentalis*) trees. *Weed Science* **32**: 320-327. DOI:10.2307/2F4043941.

TABLES

1. Table 1: SHAW above-ground parameter changes across the three vegetation simulations: juniper, mountain big sagebrush, and low sagebrush.

Vegetation	LAI	Height (m)	Vegetation albedo
Juniper	3.0	2.5	0.10
Mtn Sagebrush	0.9	0.77	0.25
Low Sagebrush	0.3	0.18	0.25

2. Table 2: SWI amount and timing for current and future climates for the two eight-year periods. SWI 50% is WY day when 50% of Oct-June SWI occurred. Numbers in parentheses denote standard deviation. Snow disappearance (disap.) day is calculated based on the first day without snow after February 1st. Evaporation-Sublimation (ES) loss is the average annual loss.

	Snow disap. day - current	**Snow disap. day - future**	**SWI-current (mm)**	**SWI-future (mm)**	**SWI 50% - current (days)**	**SWI 50% - future (days)**	**ES loss -current (mm)**	**ES loss -future (mm)**
Juniper	103 (21)	47 (18)	390 (109)	377 (103)	178 (18)	132 (17)	213 (16)	229 (19)
Mtn. sage	104 (20)	52 (21)	511 (121)	492 (112)	183 (18)	142 (14)	114 (16)	138 (10)
Low sage	105 (19)	59 (18)	545 (118)	535 (116)	185 (18)	137 (16)	123 (22)	142 (23)

FIGURES

1. **Figure 1**: Lysimeter-derived throughfall for snow ($TF_{snow,l}$), mixed (TF_{mixed}), and rain (TF_{rain}), and snow depth derived throughfall ($TF_{snow,d}$), relative to total storm lysimeter output (rain/snowmelt) or snow depth (P_G).

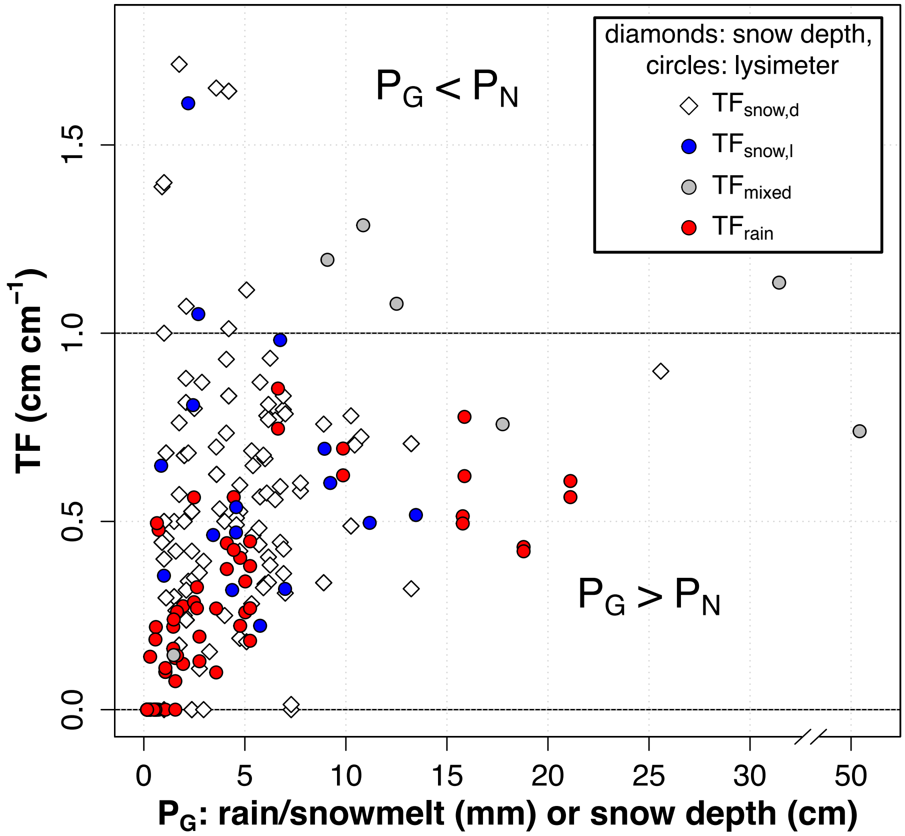

2. **Figure 2**: Snow depth throughfall ($TF_{snow,d}$) across snow events with a range of pre-event differences in snow depth between the interspace and under the tree ($D_{tree\text{-}inter}$), with increasing values representing greater depth of snow in the interspace than under the tree. Circle size denotes interspace storm snow depth.

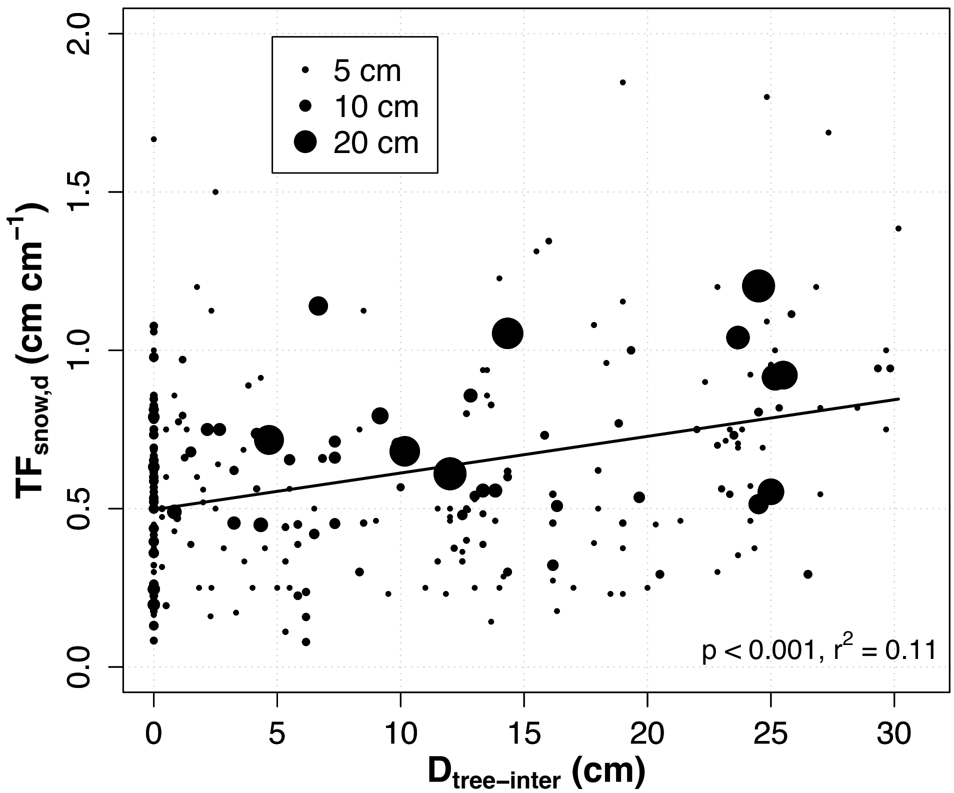

3. Figure 3: The (a,b,c) Canopy storage (S) and (d,e,f) evaporation rate ($\overline{E}/\overline{R}$) estimated with the Gash analytical model for rain events. Canopy storage and $\overline{E}/\overline{R}$ are plotted against (a,d) event size (P_G), (b,e) wind speed (u), and (c,f) vapor pressure deficit (VPD). Circle size in u and VPD plots correlate to event size.

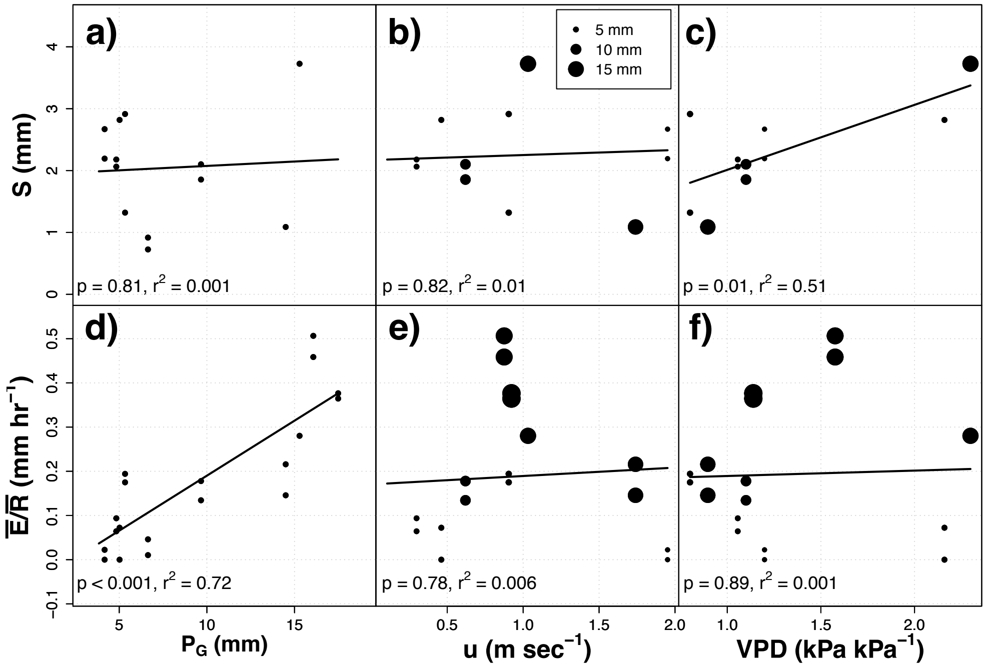

4. **Figure 4**: Rain interception loss (I_{rain}) from the beginning to the end of the growing season. Circle size denotes event size.

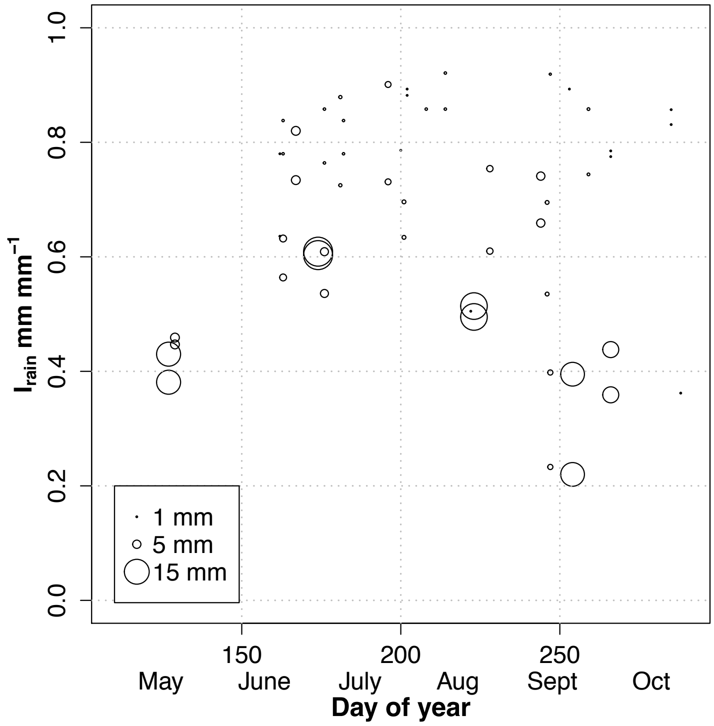

5. **Figure 5:** Average snow depth in interspace (brown) and under tree (green) for A) WY 2013 and B) WY 2014. Bold line is the average and outside border of the shaded region is the maximum and minimum snow depth. Circles are average snow survey snow depth under trees and in the interspace and error bars are one standard deviation. No average was plotted for WY 2013 due to a camera failure and only two stakes for both the interspace and canopy.

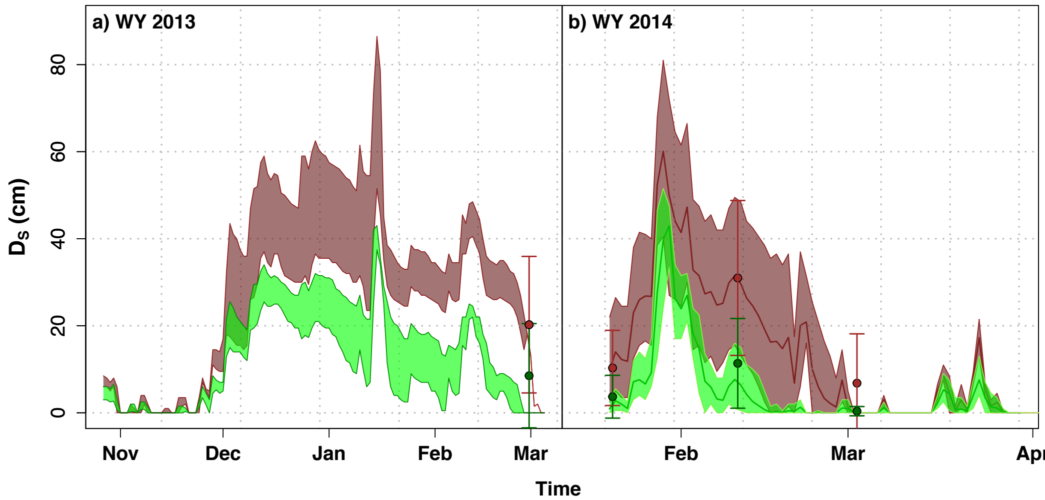

6. **Figure 6:** Ratio of total monthly precipitation falling as snow (SWE) to total monthly precipitation (P_G) over WY 2007-2014 (blue circles) and under mid-21st century warming (red squares). Points are averages for the eight-year period, error bars denote one standard deviation.

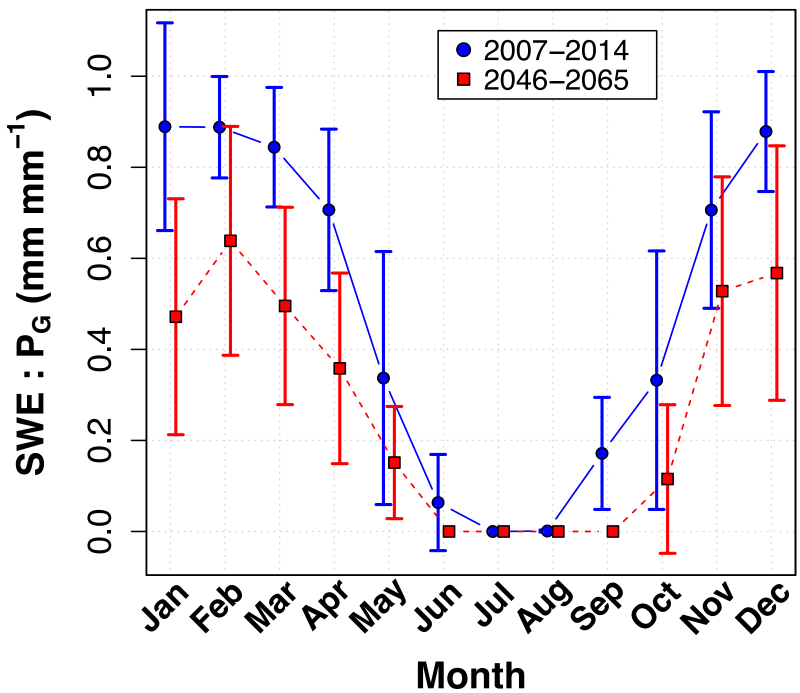

7. **Figure 7**: Average SWE for WY 2007-2014 (solid) and an 8 year period based on the projected climate in 2045-2064 (dotted line). Plots are for A) juniper, B) mountain big sagebrush, C) low sagebrush where bold line represents SWE through time averaged over the 4 years middle peak SWE years, and lines above (below) represent the two years with the highest (lowest) peak SWE accumulation. Panel D) compares average juniper (bold) and mountain big sagebrush (not bold) SWE for current climate (solid) and 8 year period based on 2045-2064 future climate (dotted).

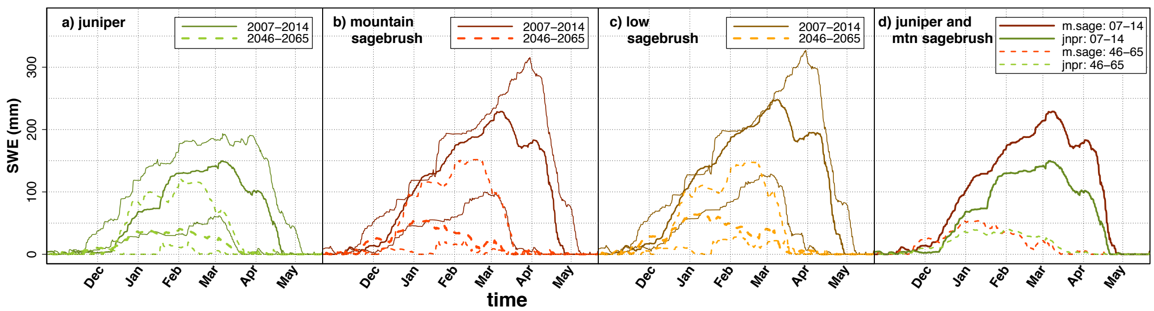

8. **Figure 8**: Plots of (a,b,c) monthly surface water input (SWI) and (d,e,f) monthly canopy and soil surface evaporation and sublimation (ES) loss in juniper, mountain big sagebrush, and low sagebrush over WY 2007-2014 (current climate) and WY 2046-2065 (future climate). Darker (lighter) colors, circles (squares), and solid (dotted) lines signify current (future) climate. Points are averages for the given period, error bars denote one standard deviation.

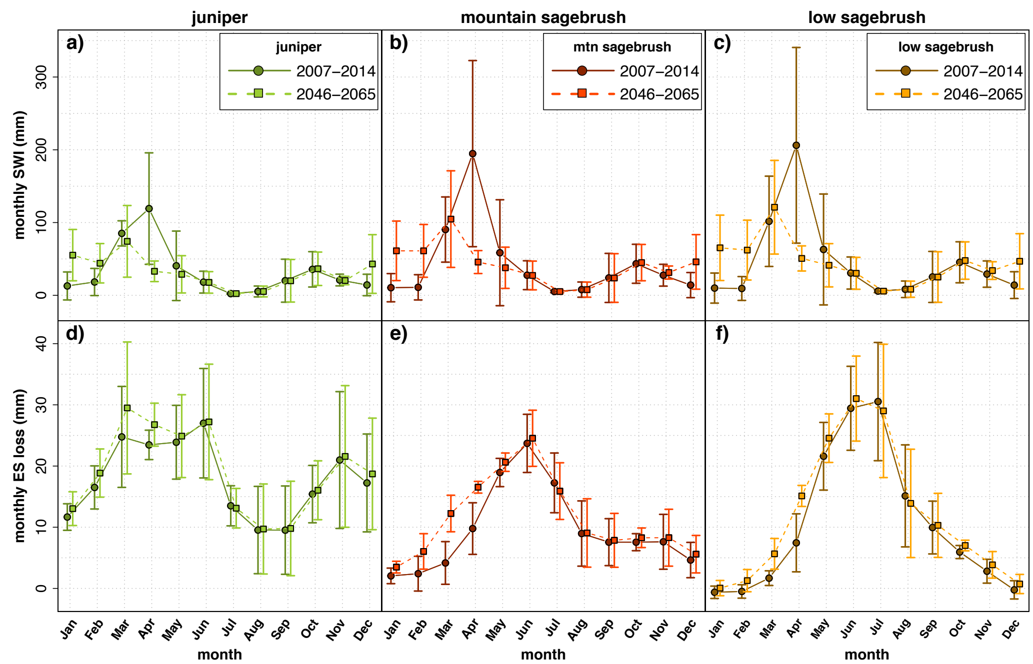

9. **Figure 9**: The (a) total annual surface water input (SWI) and (b) day of year of 50% SWI (SWI 50% day) vs. annual peak snow water equivalent (SWE). Color denotes the spectrum of November – March temperature with white being zero, colors above zero as red and below zero as blue. Shapes denote vegetation with circles denoting low sagebrush, squares denoting mountain big sagebrush, and triangles denoting juniper. Solid shapes are WY 2007-2014 (current climate) and hollow shapes are under mid-21st century warming (future climate). Blue (red) regression lines are for years with November – March temperatures below (above) 0° C.